

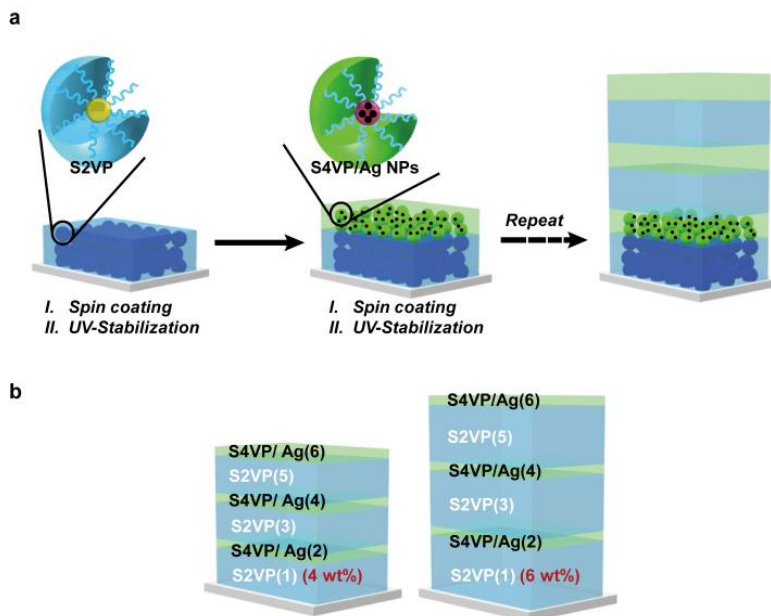
Supporting Information

Periodic Layered Inverse Micelle Multilayers with Tunable Photonic Band Gap: Fabrication and Application in Dye-Sensitized Solar Cells

Yoon Hee Jang and Dong Ha Kim *

Department of Chemistry, Global Top 5 Research Program, Ewha Womans University, 52, Ewhayeodae-gil, Seodaemun-gu, Seoul, 120-750, South Korea

Fabrication of BCP Multilayer Composed of S2VP and S4VP/Ag Alternating Layers



Scheme S1. a) Schematic illustration for hybrid layered nanostructures fabricated by stepwise layer-by-layer assembly of UV-stabilized BCP inverse micelles. b) BCP layered structures fabricated from 4% or 6% S2VP solutions and relatively dilute S4VP solution containing Ag precursors.

The hybrid layered BCP structures containing silver NPs as inorganic counterpart were fabricated *via* UV-stabilized BCP stacking. Overall procedures are illustrated in Scheme S1.

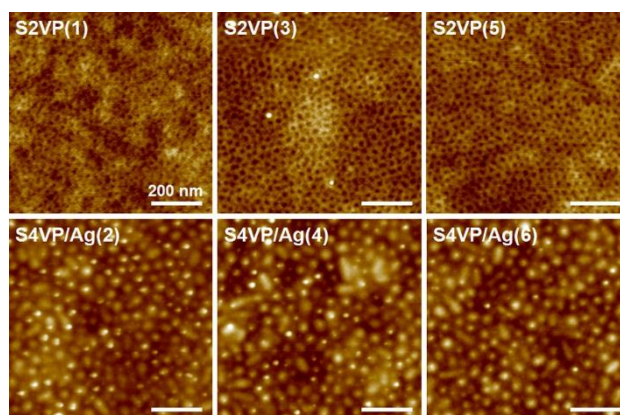


Fig. S1 AFM height images of each constituting layer of [S2VP/(S4VP/Ag)]₆ after UV-stabilization.

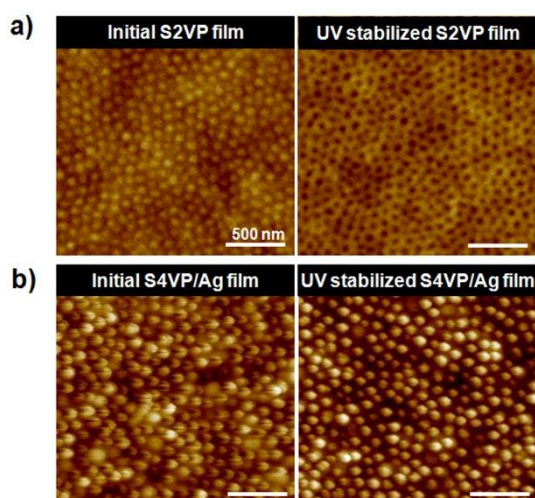


Fig. S2 AFM height images of a) initial (left) and UV stabilized (right) S2VP film, b) initial (left) and UV stabilized (right) S4VP/Ag film.

A series of height-contrast AFM images of [S2VP/(S4VP/Ag)]₆ were shown in Fig. S1. The upper and lower panels in Fig. S1 display surface morphologies of S2VP layers and S4VP/Ag layers after UV exposure for 1 h, respectively. In comparison to the pristine spherical reverse S2VP micelles, dark hole was observed at the positions of the P2VP core (Fig. S2(a)) after UV exposure. The initial S2VP reverse micelles film was transformed into nanoporous structure by selective degradation of P2VP core and cross-linking of PS corona during UV exposure. On the other hand, both PS and P4VP blocks were stabilized, since Ag precursors were selectively incorporated with pyridine unit of P4VP through coordination bond (Fig. S2(b)).

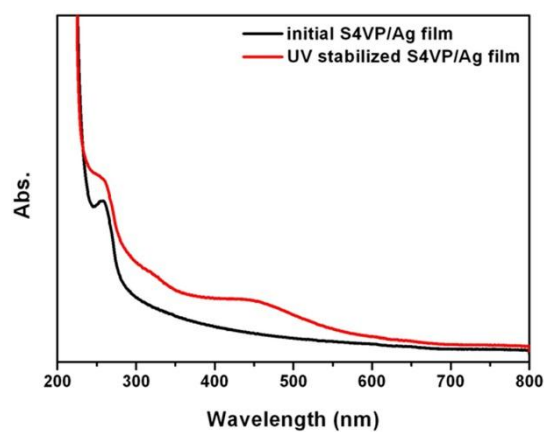


Fig. S3 UV-Vis absorption spectra of initial (black curve) and UV stabilized (red curve) S4VP/Ag film. Samples for UV-Vis absorption spectra were prepared on quartz substrates.

Furthermore, a characteristic surface plasmon resonance band of Ag NPs at around 450 nm proved that Ag precursors were concurrently reduced to metallic Ag NPs under illumination of UV light (Fig. S3).

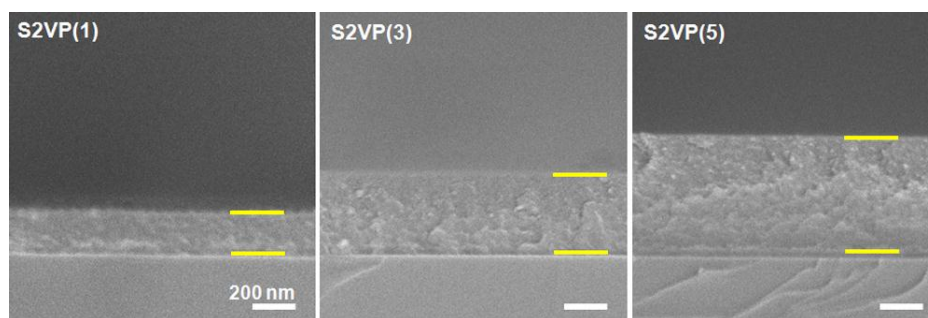


Fig. S4 Cross-sectional SEM images of 4 wt% S2VP layers: S2VP (1), (3) and (5).

Stepwise deposition of stabilized BCP films was confirmed by scanning electron microscopy (SEM) and the thickness of each layer was measured by using alpha step. The thickness of S2VP (4%) layer was about 150 ± 10 nm and total thickness was about 500 ± 10 nm. Cross-sectional SEM (Fig. S4) revealed that the thickness of the film was gradually increased with increasing the number of S2VP layer, indicating that the BCP reverse micelles were successfully stacked through UV-stabilization and subsequent layer deposition. However, the thin layer of S4VP/Ag (about 40 nm) was barely distinguishable in the SEM because of similar secondary electron release property between S2VP and S4VP although S4VP contains Ag NPs.

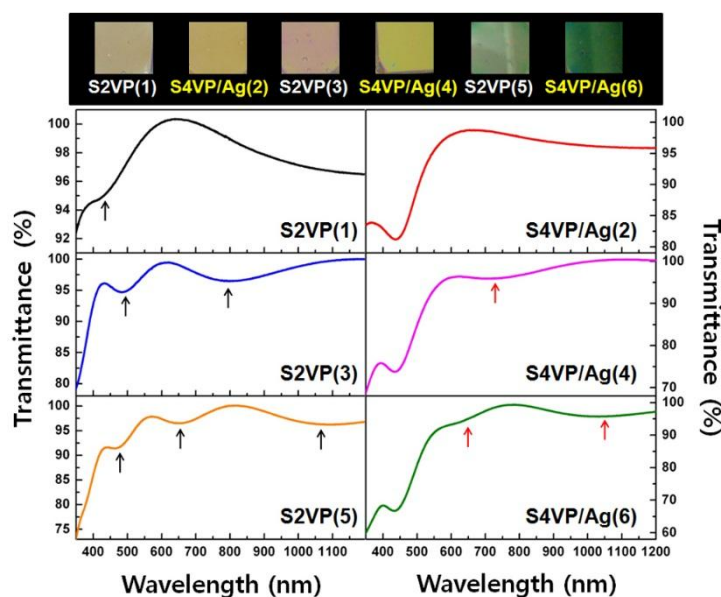


Fig. S5 Color variations of $[S2VP(4\%)/(S4VP/Ag)]_6$ with increasing the number of layer and transmittance spectra of each layer of $[S2VP(4\%)/(S4VP/Ag)]_6$ after UV-stabilization.

The multilayered BCP films show the reflective colors and these colors have changed with increasing the number of layer. The representative color alteration can be attributed to the interference between the periodic layers. Fig. S5 shows the transmittance spectra of each layer of $[S2VP(4\%)/(S4VP/Ag)]_6$. As shown in Fig. S5, number of oscillations (it is commonly known as Fabry-Perot oscillations) increases and gradually shifts to the higher wavelength with increasing the number of S2VP layer (black arrows in the left panel in Fig. S5). Spectra bandwidth in the range of the longest wavelength was also gradually broadened, which might be inferred from increased interference. Meanwhile, when thin S4VP/Ag layer was deposited, the transmission dip in the shortest wavelength region disappeared and others were broadened relative to the former S2VP layer (red arrows in the right panel in Fig. S5). The specific peak is also observed at around 450 nm in S4VP/Ag layer, which originates from reduced Ag NPs and consistent with typical surface plasmon band of Ag NPs.

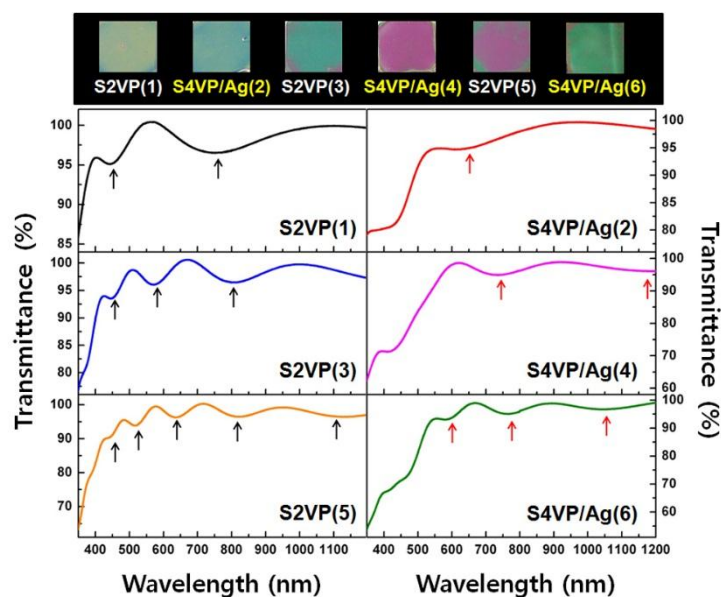


Fig. S6 Color variations of $[S2VP(6\%)/(S4VP/Ag)]_6$ with increasing the number of layer and transmittance spectra of each layer of $[S2VP(6\%)/(S4VP/Ag)]_6$ after UV-stabilization.

The color variations and the transmittance spectra of $[S2VP(6\%)/(S4VP/Ag)]_6$ display a similar tendency (Fig. S6), but it was more complicated owing to the larger periodic size. It should be noted from these results that (1) layered BCP structures fabricated via stepwise layer-by-layer assembly have long-range order, which was substantiated by exhibiting higher order peak; (2) the oscillations of these layered BCP can be tunable in the wavelength range from the UV region to the near IR region; (3) the position and number of oscillations can be diversified by controlling the inner architectures of layered BCP film. However, there was no observation of photonic crystal property (such as photonic stop bands at specific wavelength) due to the not much difference in refractive indices between S2VP ($n \approx 1.59$) and S4VP/Ag ($n \approx 1.61$) layers.